

## Article

# The General Relationship between Mean Dissolved Oxygen Concentrations and Timescales in Estuaries

Jian Shen <sup>1,\*</sup>  and Qubin Qin <sup>2</sup><sup>1</sup> Virginia Institute of Marine Science, William & Mary, Gloucester Point, VA 23062, USA<sup>2</sup> Coastal Studies Institute, East Carolina University, Wanchese, NC 27981, USA; qinq23@ecu.edu

\* Correspondence: shen@vims.edu

**Abstract:** The onset of hypoxia is a consequence of the competition between oxygen replenishment, production, and consumption. Dissolved oxygen (DO) levels inside an estuary depend on the balance between physical processes that transport oxygen-rich water into the estuary, including upstream freshwater advection, gravitational circulation, and vertical mixing, and biochemical processes that produce and consume oxygen, such as photosynthesis, respiration, and organic decomposition. We propose a general relationship between the physical and biochemical processes with a Lagrangian perspective to interpolate mean DO concentrations at local and system levels to assess the onset of hypoxia in an estuary. Simple parameters using timescales are proposed for cross-system comparison of hypoxia and anoxia conditions. Our study demonstrates that the hypoxia of an estuary system is determined by the timescales of vertical exchange, freshwater and saltwater transport, and DO consumption. When the vertical exchange timescale is shorter than the residence time in a system, vertical exchange dominates DO replenishment, while shorter residence time enhances advection, which quickly inputs DO-rich water to regulate hypoxia. The interplay between DO consumption and dynamic DO replenishment is the primary determinant of hypoxia in an estuary.

**Keywords:** hypoxia and anoxia; cross-system comparison; transport timescales; vertical exchange time; residence time; Chesapeake Bay



**Citation:** Shen, J.; Qin, Q. The General Relationship between Mean Dissolved Oxygen Concentrations and Timescales in Estuaries. *Water* **2024**, *16*, 969. <https://doi.org/10.3390/w16070969>

Academic Editor: Giuseppe Oliveto

Received: 28 February 2024

Revised: 21 March 2024

Accepted: 21 March 2024

Published: 27 March 2024



**Copyright:** © 2024 by the authors. Licensee MDPI, Basel, Switzerland. This article is an open access article distributed under the terms and conditions of the Creative Commons Attribution (CC BY) license (<https://creativecommons.org/licenses/by/4.0/>).

## 1. Introduction

Hypoxia and anoxia are phenomena characterized by dissolved oxygen (DO) levels falling below  $2 \text{ g O}_2 \text{ m}^{-3}$  and reaching zero, respectively. Persistent seasonal hypoxia occurs in many stratified or partially mixed estuaries and shelf regions worldwide [1–4]. It causes water degradation, which is harmful to living resources, kills fish, and causes the deterioration of water quality [1,4]. Hypoxia and anoxia occur when oxygen consumption exceeds oxygen production and replenishment within an aquatic environment. In the context of an estuary, DO replenishment occurs through vertical and lateral mixing processes, advection of upstream freshwater, or gravitational circulation (exchange flow) that transports DO-rich water into the estuary [2,3]. Conversely, oxygen production/consumption mainly result from phytoplankton photosynthesis/respiration, nitrification, organic matter decomposition, and bottom sediment oxygen demand (SOD). Because of the persistence of estuarine stratification, hypoxia often develops in sub-pycnocline water when the DO consumption rate of biochemical processes surpasses the oxygen supply [2]. Hypoxia occurs in rivers and coastal waters, and its frequency of occurrence appears to be increasing and is most likely accelerated by human activities [1,4]. The phenomenon of low-DO conditions in aquatic ecosystems has captured the interest of researchers and managers. Understanding the causes of hypoxia and effectively managing them is an urgent need and it requires a multidisciplinary approach.

Because the transport and mixing processes play a crucial role in modulating DO, physical oceanographers have become increasingly interested in the dynamics of oxygen

variations and how they modulate DO dynamics. In the Chesapeake Bay, it has been found that freshwater discharge is a major factor in regulating stratification [5], which is a predictor of summertime hypoxic volume due to high nutrient input during spring runoff [6]. Kuo and Neilson [3] analyzed DO budgets in the Virginia tributary estuaries of the Chesapeake Bay. They pointed out the importance of gravitational circulation in modulating DO in these tributaries. In addition to gravitational circulation, Sanford et al. [7] showed the importance of the lateral exchange of DO between the surface and sub-pycnocline water due to lateral circulations. Scully [8] demonstrated that wind plays a crucial role in modulating hypoxia in the Chesapeake Bay through lateral circulation. Because of the complicity of dynamics, this makes cross-system comparison challenging.

The approach of using timescales for understanding the overall effect of dynamics and transport processes has been used for cross-system comparison under a common currency [9–12]. Shen et al. [10] provided a simplified two-layer theoretical model, for which the bottom DO concentration can be interpolated by the timescales of vertical exchange time ( $\tau_v$ ), horizontal transport time (saltwater age), and DO consumption time. The timescale approach was verified by a three-dimensional model in the Chesapeake Bay [13]. Recently, Fennel and Testa [14] proposed a non-dimensional number that relates the hypoxia timescale and water residence time to guide the cross-system comparison, which provides a convenient method of cross-system comparison. However, the water residence time does not account for the vertical exchange that is a key parameter for DO replenishment [2,7] when the water residence time is long [10]. The competition between vertical and horizontal transport needs to be quantified and included to fully account for the DO dynamics.

The purpose of this study is to provide a general relationship between DO and transport timescales in estuaries, using a Lagrangian perspective, to quantify the effects of physical and biochemical processes on the mean DO at both local and system scales, which can be used to assess the onset of hypoxia in an estuary and enable cross-system comparisons. While the simplified approach is based on an idealized estuary, it provides insights into understanding DO dynamics. This study demonstrates that the hypoxia of an estuary system can be effectively quantified by timescales, which can be used for cross-system comparison.

## 2. Methods

In this section, a general case that is applicable to both rivers and estuaries is introduced to understand the relationship between physical and biochemical processes that influence the average DO levels in these environments. We derived simple relationships between mean DO and DO replenishment/net consumption in a river or estuary with the ultimate objective of describing the interplay between physical and biological processes while acknowledging that the various processes influencing DO variation in an estuary are inherently spatially and temporally variable over finer scales.

### 2.1. DO Variation along a River or Estuary

To study DO variation along a river or an estuary and the relationship between DO variation and timescales, we assume that the estuary or river can be represented by a rectangle channel with the constant cross-section area  $A$  ( $\text{m}^2$ ) and depth  $H$  (m) for simplicity without losing generalization. The mass balance of DO (tidally averaged for estuary), which is similar to the salt balance, can be expressed as [15–17]:

$$O_t + \frac{1}{A}(uAO)_x + (wO)_z = \frac{1}{A}(k_H O_x A)_x + (k_z O_z)_z + P - R, \quad (1)$$

where  $O$  ( $\text{g O}_2 \text{ m}^{-3}$ ) is the DO concentration at a specific location  $(x, z)$  and time  $(t)$ ,  $u$  and  $w$  ( $\text{m s}^{-1}$ ) are the horizontal and vertical velocities at location  $(x, z)$ , respectively;  $k_H$  and  $k_z$  ( $\text{m}^2 \text{ s}^{-1}$ ) are the horizontal and vertical diffusivity, respectively; and  $P$  and  $R$  ( $\text{g O}_2 \text{ m}^{-3} \text{ s}^{-1}$ ) are DO production and total consumption rates, respectively. Using the boundary conditions

$k_z \frac{dO}{dz}(z = 0) = \theta_s$  and  $k_z \frac{dO}{dz}(z = -H) = \theta_b$ , where  $\theta_s$  and  $\theta_b$  are the surface and bottom DO fluxes ( $\text{g O}_2 \text{ m}^{-2} \text{ s}^{-1}$ ), respectively [17], the vertical mean DO can be expressed as:

$$\bar{O}_t + \frac{1}{A}(\bar{u}A\bar{O})_x + \frac{1}{A}(\bar{u}'O'A)_x = \frac{1}{A}(k_H\bar{O}_x A)_x + \bar{P} - \bar{R} + \frac{1}{H}(\theta_s - \theta_b). \tag{2}$$

Under the steady-state assumption (i.e.,  $\bar{O}_t = 0$ ), and assuming that  $\frac{1}{A}(k_H\bar{O}_x A)_x$ , and  $\frac{1}{A}(\bar{u}'O'A)_x \ll \frac{1}{A}(\bar{u}A\bar{O})_x$ , the dominant advection terms of the vertical mean  $\bar{O}$  can be expressed as (hereafter, we dropped the over bar of all variables for convenience):

$$uO_x = P - \left(R + \frac{\theta_b}{H}\right) + \frac{1}{H}\theta_s. \tag{3}$$

Using the boundary condition and assuming  $k_z$  is independent of depth,  $\theta_s$  can be approximated as follows:

$$\frac{\theta_s}{k_z} = \frac{dO}{dz} \approx \frac{O_s - O}{h}, \tag{4}$$

Here, we scaled the flux  $\theta_s$  by using the difference between DO at the surface ( $O_s$ ) and mean  $O$  at the water depth of  $h$  below the surface at location  $x$ .  $O_s$  can be higher, lower, or equal to saturation DO. Using Equation (4), the last term of Equation (3) can be written as  $\frac{k_z}{Hh}(O_s - O)$ . Note that  $Hh/k_z$  is a vertical mixing timescale. Although  $h$  is not readily determined, the mixing scale can be obtained from model simulations of surface water age [10], which will be further discussed. We refer to this timescale as vertical exchange time ( $\tau_v$ ),  $\tau_v = Hh/k_z$ , which quantifies how long it will take for surface water with high DO to be transported to the location  $x$ . By substituting Equation (4) into Equation (3), Equation (3) can be written as:

$$\frac{dO}{dx} + \frac{O}{u\tau_v} = -\frac{R_N}{u} + \frac{O_s}{u\tau_v}, \tag{5}$$

where  $R_N = \left(R + \frac{\theta_b}{H} - P\right)$ , in which  $R_N$  is the net DO consumption rate, resulting from water column respiration, production, and bottom sediment oxygen demand [10]. Note that  $-R_N$  is net ecosystem metabolism (NEM) and  $R_N$  can be either positive or negative, which can be estimated through measurements. A positive  $R_N$  indicates that respiration is larger than production and vice versa. If we assume the upstream boundary  $O = O_u$  at  $x = 0$ , the solution of Equation (5) is:

$$O = [O_u - (O_s - \tau_v R_N)]e^{-\frac{x}{\tau_v}} + O_s - \tau_v R_N \tag{6}$$

where  $\tau_u = x/u$  is the time required for freshwater travel from the upstream boundary to the location  $x$  (i.e., residence time [9,18,19]), which can be estimated by freshwater age [18,19]. The first term on the right side of Equation (6) is the deficit of DO consumption due to upstream DO advection, and the last term is the DO consumed during the period of vertical transport. Equation (6) indicates that the mean DO concentration at location  $x$  is a superimposition of DO advection from the upstream and vertical mixing. When  $\tau_u$  is large (slow-moving water), the first term vanishes, indicating that the DO-rich water transported from the upstream boundary has been depleted and has less impact on DO dynamics at the present location.

In estuaries, DO-rich water can also enter from the outside through gravitational circulation [3]. The DO input with saltwater has the same effect as freshwater on DO. Therefore, the general solution can be expressed as the superimposition of the horizontal DO transport from the upper stream, downstream, and surface as:

$$O = O_s - \tau_v R_N + [O_u - (O_s - \tau_v R_N)]e^{-\frac{\tau_u}{\tau_v}} + [O_d - (O_s - \tau_v R_N)]e^{-\frac{\tau_d}{\tau_v}} \tag{7}$$

where  $\tau_d = x/u_e$  is the time required for saltwater to be transported to the location  $x$  in the estuary, which can be estimated by saltwater age [10];  $u_e$  is the exchange flow;  $O_d$  is the DO concentration at the downstream boundary; and  $\tau_R = 1/R_N$  is the timescale for net DO consumption. Note that DO transport from the upstream or downstream boundary is modulated by the vertical exchange timescale. If  $\tau_v$  is relatively short ( $\tau_v \ll \tau_u$  or  $\tau_d$ , i.e., slow horizontal transport), the effect of the transport of DO-rich water from the upper stream and downstream becomes negligible. When  $\tau_v \gg \tau_u$  or  $\tau_d$ , DO transported from the upstream or downstream boundary dominates the DO replenishment. By introducing timescales, we presented the solution from a Lagrangian perspective, where DO can be assessed at each observational location using a common currency [9]. Therefore, DO concentration can be expressed by the horizontal freshwater and saltwater ages, vertical exchange times of water, and net DO consumption time at the observational locations.

For a special case when  $O_u = O_d = O_s = O_{sa}$ , i.e., when DO concentrations at the boundaries are all equal to the saturated DO concentration ( $O_{sa}$ ), Equation (7) can be simplified as:

$$O = O_{sa} - O_{sa} \tau_v / \tau'_R (1 - e^{-\frac{\tau_u}{\tau_v}} - e^{-\frac{\tau_d}{\tau_v}}). \quad (8)$$

The normalized  $O$  distribution is

$$\frac{O}{O_{sa}} = 1 - \frac{1}{\tau_R^*} (1 - e^{-\tau_{eu}^*} - e^{-\tau_{ed}^*}), \quad (9)$$

where we define  $\tau'_R = \frac{O_{sa}}{R_N}$  as a timescale for net DO consumption and the dimensionless timescale parameters  $\tau_{eu}^* = \frac{\tau_u}{\tau_v}$ ,  $\tau_{ed}^* = \frac{\tau_d}{\tau_v}$ ,  $\tau_R^* = \frac{\tau'_R}{\tau_v}$ . Figure 1 shows the contours of DO variations with respect to  $\tau_{eu}^*$  and  $\tau_{ed}^*$  (there is a similar DO distribution for the upper boundary  $\tau_{eu}^*$  and  $\tau_R^*$ ). A decrease in  $\tau_{ed}^*$  (i.e., an increase in DO consumption rate) increases the chance of hypoxia, while an increase in gravitational circulation or freshwater discharge (i.e., a decrease in  $\tau_{eu}^*$  or  $\tau_{ed}^*$ ) improves DO conditions inside the estuary for a given  $\tau_v$  (Figure 1a). The onset of hypoxia depends on the ratio of DO consumption and vertical exchange and horizontal transport times. DO concentrations at the boundary affect DO concentrations inside the estuary, and incoming water with low DO concentration (e.g.,  $O_d = 0.5 O_{sa}$ ) results in a decrease in estuarine DO concentrations (Figure 1b). This impact varies with saltwater age. When saltwater age is low at a location, either due to a short distance from the downstream boundary or a high exchange flow, low-DO water at the mouth of the estuary is transported into the location quickly, and the incoming water with lower DO concentrations significantly decreases DO concentrations at that location. However, DO at the downstream boundary has a low impact on local DO dynamics at a location where saltwater age is high, as most incoming DO from the downstream boundary has been consumed before reaching that location.

## 2.2. Timescales Controlling Hypoxia in a System

If we assume the waterbody is well mixed with a volume  $V$  ( $\text{m}^3$ ) and surface area  $A$  ( $\text{m}^2$ ), it has one principal opening to transport water out. Inflows to the system occur through estuarine circulation that moves water into the system from its opening. DO input to the system can be from the upstream and downstream boundaries as well as through the surface exchange, and DO consumption is proportional to the volume of the waterbody. We acknowledge that this is an overly simplified system. The purpose of this analysis is to understand the interplay between physical transport processes and DO consumption at a system-wide scale. With these assumptions, the vertical-averaged mass balance under the steady state over a specified averaging period  $T$  (e.g.,  $T =$  tidal cycle, or day) can be simplified under the steady state and can be written as follows [11]:

$$(Q_{in} + Q_r)O_{sa} - Q_e O - R_N V + \frac{k_z}{h} (O_{sa} - O)A = 0, \quad (10)$$

where  $O$  is the mean oxygen of the waterbody ( $\text{g O}_2 \text{ m}^{-3}$ ) and  $O_{sa}$  is DO saturation ( $\text{g O}_2 \text{ m}^{-3}$ ). Here, we use  $O$  as the system mean DO for convenience rather than the DO at location  $x$  as in Equation (5).  $Q_{in}$  is the inflow ( $\text{m}^3 \text{ d}^{-1}$ ) at the downstream boundary,  $Q_r$  is the freshwater discharge,  $Q_e$  is the outflow ( $\text{m}^3 \text{ d}^{-1}$ ) at the downstream boundary, and  $Q_e = Q_{in} + Q_r$  [11]. Here, we assume the DO inputs from upstream, downstream, and the surface are at saturation. The first two terms are advection terms.  $R_N$  is the net respiration rate ( $\text{g O}_2 \text{ m}^{-3} \text{ d}^{-1}$ ) as defined before. The last term of Equation (10) is the approximation of DO exchange between the waterbody and surface water with a DO concentration equal to  $O_{sa}$  (Equation (4)). Assuming that volume does not change, Equation (10) can be written as:

$$Q_e(O_{sa} - O)/V - R_N + \frac{k_z}{Hh}(O_{sa} - O) = 0. \tag{11}$$

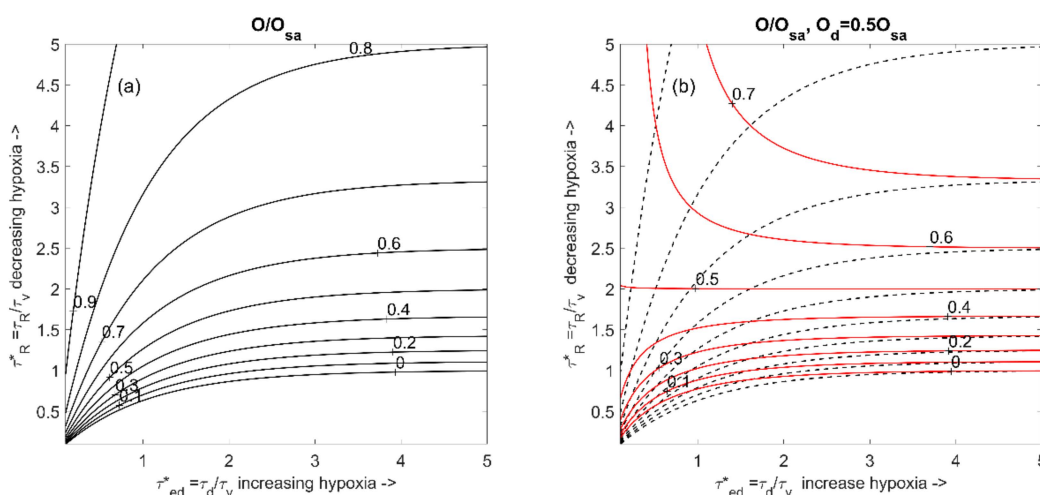


**Figure 1.** Change in normalized DO with respect to non-dimensional physical and biological timescale parameters (only shows DO influence from the mouth,  $\tau_{ed}^*$ ). Panel (a) shows that an increase in net DO consumption rate (decreased  $\tau_R^*$ ) increases the chance of hypoxia, while an increase in gravitational circulation (decreased  $\tau_{ed}^*$ ) improves the DO conditions inside the river or estuary for a given vertical exchange time. Panel (b) shows that when DO outside of a waterbody is low, it can affect the DO inside the estuary, resulting in a decrease in DO concentrations (red lines).

Note that the term  $V/Q_e$  is the residence time [11,20]. Let  $\tau = V/Q_e$ , and  $\tau_v = Hh/k_z$  as the residence and vertical exchange times, respectively. Equation (11) can be expressed as:

$$O\left(\frac{1}{\tau} + \frac{1}{\tau_v}\right) = O_{sa}\left(\frac{1}{\tau} + \frac{1}{\tau_v}\right) - R_N. \tag{12}$$

The mean DO in the waterbody can be expressed as

$$O = O_{sa} - R_N \left(\frac{\tau_v}{1 + \frac{\tau_v}{\tau}}\right) \text{ or } O = O_{sa} - R_N \left(\frac{\tau}{1 + \frac{\tau}{\tau_v}}\right). \tag{13}$$

Equation (13) shows two typical cases, for which  $O = O_{sa} - R\tau_v$  if  $\tau_v \ll \tau$ , or  $O = O_{sa} - R\tau$  if  $\tau \ll \tau_v$ . For a large waterbody in which  $\tau$  is much longer than  $\tau_v$ , such as the Chesapeake Bay, DO is mainly controlled by  $\tau_v$ , except in the regions near the headwater or near the mouth. For a small waterbody with a short residence time, DO can be renewed by transporting DO-rich water from its boundaries, either from its upper stream or downstream. Although the system is simplified, the result (Equation (13)) provides the key relationship between DO transport and net DO consumption. Given  $R_N$ ,  $\tau_v$ , and  $\tau$ , the hypoxic condition of a waterbody can be determined. Although the model

is derived for the whole system, the relationship is applicable to a segment of a river or estuary to assess local DO in a sub-region, which provides a more accurate estimation.

### 2.3. Compute Vertical Exchange Time and Water Ages

To demonstrate the use of timescales to determine DO, we used the Chesapeake Bay as an example. The Environmental Fluid Dynamics Code (EFDC) [21,22] was applied to the Chesapeake Bay to simulate hydrodynamics and transport timescales. The EFDC uses a boundary-fitted curvilinear grid model in the horizontal and sigma grids in the vertical. This model was calibrated for the surface elevation, current, and salinity of the Chesapeake Bay [13]. The model produced reliable stratification and destratification responses temporally and spatially in both wet and dry years. The grid is shown in Figure 2a. The model is forced by the interpolated observed tide at the open boundary (<http://tidesandcurrents.noaa.gov>, accessed on 20 March 2024), freshwater discharges of eight main tributaries (<http://waterdata.usgs.gov/nwis/>, accessed on 20 March 2024), and wind obtained from the North America Regional Reanalysis (NARR) produced at the National Center for Environmental Prediction (<https://psl.noaa.gov/data/gridded/data.narr.html>, accessed on 23 March 2024). The climatology salinity data were used at the open boundary.

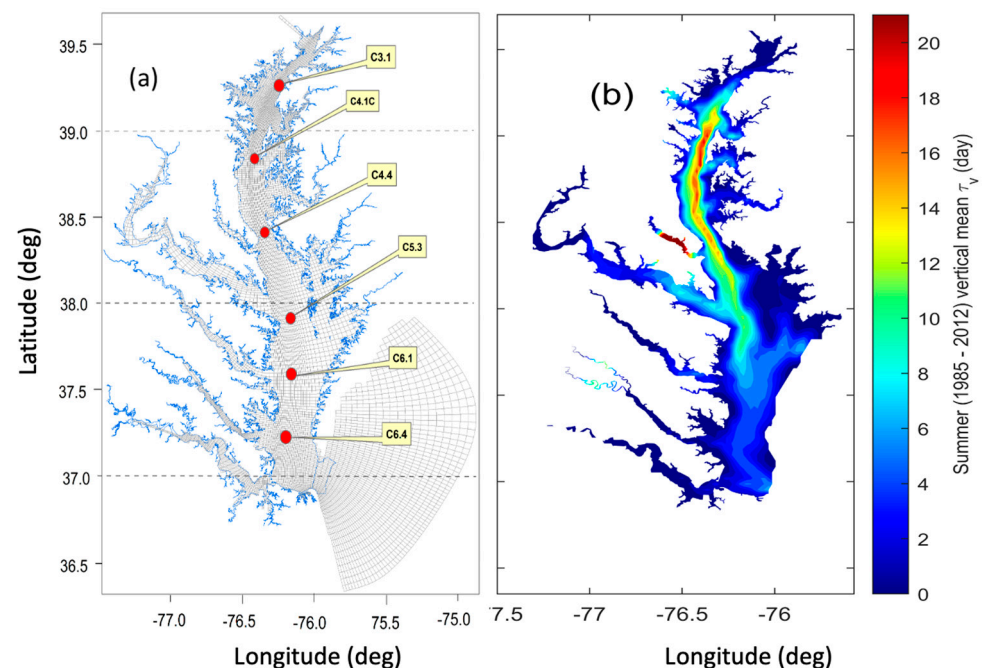


**Figure 2.** (a) Model grid of the Chesapeake Bay and observational stations (red dots). (b) Average summer (1985–2012) vertical mean transport time ( $\tau_v$ ).

The Constitutional-oriented Age and Residence Time Theory (CART) [18,19] was applied to compute various water ages corresponding to vertical exchange time,  $\tau_v$ , freshwater transport time (freshwater age  $\tau_u$ ), and saltwater transport time (saltwater age  $\tau_d$ ). The  $\tau_v$  was computed using the water age of the surface water by continuously releasing dye at the surface and setting the age concentration to be zero at the surface [23]. The transport time of freshwater and saltwater from the open boundary was computed by releasing dye at the freshwater inflows and open boundary, respectively [24]. The age at freshwater inflow location and open boundary are set to be zero, respectively. It should be noted that  $\tau_v$  represents the age of water parcels that can be transported vertically and laterally, and can come from both upstream freshwater and saltwater when the water parcels touch the surface during the transport. Every time, the age is set to zero when the water parcels touch the surface. Therefore, the  $\tau_v$  is the elapsed time since the last time that the parcels contact the surface [23]. Different from  $\tau_v$ , the ages of water parcels do not change even when they

contact the surface, as we need to use the freshwater and saltwater ages to represent DO transport from the boundaries.

### 3. Results

#### 3.1. Transport Timescales

The averaged summer vertical mean  $\tau_v$  distribution from 1985 to 2012 is shown in Figure 2b.  $\tau_v$  distribution shows that long  $\tau_v$  occurs in the deep change in the upper portion of the Bay. It takes approximately 20 d for the surface DO-rich water to be transported to the lower layer on average in summer in the deep channel. The area with longer  $\tau_v$  is coincident with the Bay hypoxic zone [25]. Figure 3 depicts the monthly mean ages in July for the wet flow year of 1998 and the mean flow year of 2000, respectively, for freshwater, saltwater, and surface water ( $\tau_v$ ). It can be seen that age varies under different flow years. The freshwater age becomes shorter near the surface during the wet year than the mean flow year (Figure 3a,b). With a higher freshwater input during the wet year, saltwater age also becomes shorter compared to the mean flow year (Figure 3c,d). During the wet year, the estuary becomes more stratified, and  $\tau_v$  increases compared to the mean flow year (Figure 3e,f).

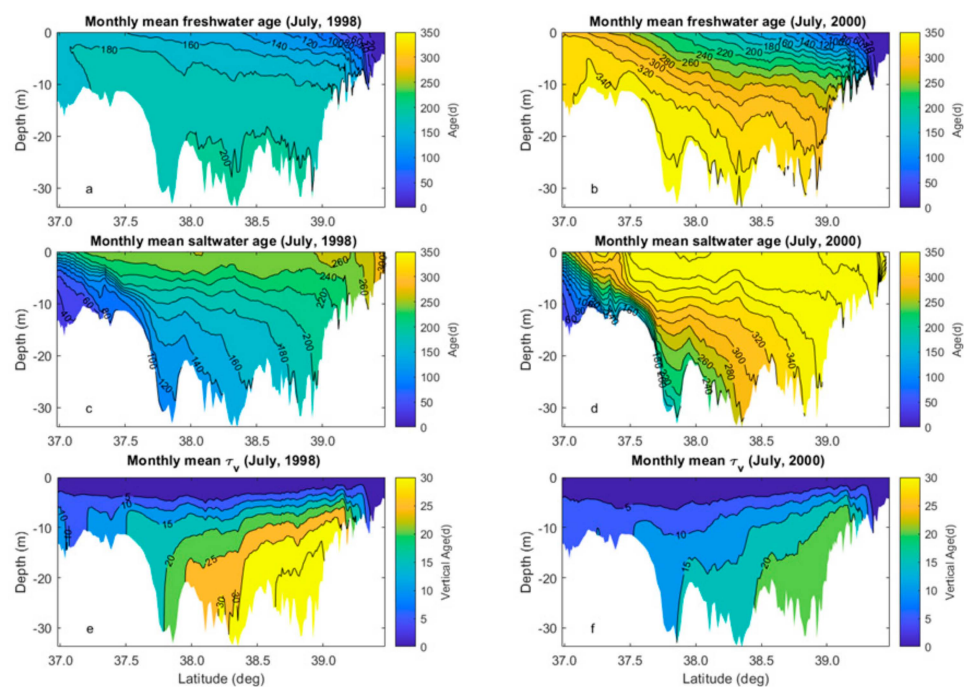


**Figure 3.** An example of model-simulated monthly mean water ages in July for a wet flow year (1998) and a mean flow year (2000) ((a,b) show freshwater age, (c,d) show saltwater age, and (e,f) show vertical exchange time,  $\tau_v$ ).

Figure 4 shows the mean vertically averaged ages for freshwater, saltwater, and surface water ( $\tau_v$ ) between 1985 and 2012 in summer along the deep channel together with their variations with one standard deviation. It takes more than 250 d for the freshwater to be transported out of the estuary. The short freshwater age (<50 d) is only located in a small region with a short distance from the discharge location in summer. It takes more than 200 d for the saltwater to be transported to the upstream in summer.  $\tau_v$  longer than 15 d is located in the region from a 38-degree to 39.25-degree latitude. The longest  $\tau_v$  is located near Station 4.1C.

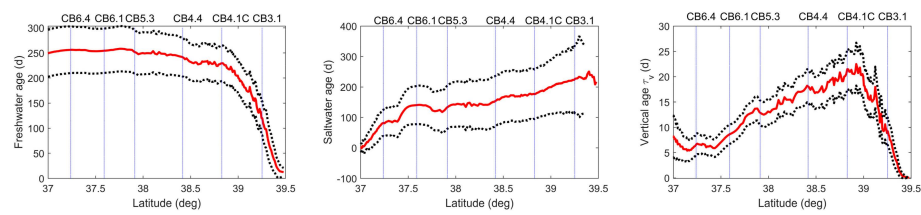


**Figure 4.** Mean vertically averaged water ages during the summer months of June to August from 1985 to 2012 (black dashed lines are one standard deviation, and station locations are marked with dashed vertical lines).

### 3.2. Dissolved Oxygen

Figure 5 shows the comparison of observed DO and modeled DO concentrations using Equation (8) at selected stations. Observational DO are monthly observations obtained from the Chesapeake Bay Program. Observation stations are shown in Figure 2. DO saturation was computed using observed temperature and salinity at each station near the surface. The net consumption rate was computed as  $R = R^{20} \theta^{T-20}$ , where  $R^{20}$  is the net respiration rate at 20 °C,  $\theta = 1.03$  [26], and  $T$  is temperature. The net DO consumption rate can be estimated as the sum of SOD and water column respiration, using an SOD value of 1.0 g O<sub>2</sub> m<sup>-2</sup> d<sup>-1</sup> for the mainstem of the Bay. This value is slightly higher than the measured high value of 0.86 g O<sub>2</sub> m<sup>-2</sup> d<sup>-1</sup> reported by Cowan and Boynton [27] but is lower than the value reported by Boynton and Kemp [28]. The mean concentration of dissolved organic carbon (DOC) in the mainstem of the Bay is about 2.0 g m<sup>-3</sup> to 4.0 g m<sup>-3</sup>. We used 2.0 g m<sup>-3</sup>, a mean DOC decay rate of 0.05 d<sup>-1</sup>, and a depth of 20 m [10,29]; the oxygen consumption rate was approximately 0.32 g O<sub>2</sub> m<sup>-3</sup>d<sup>-1</sup>, or 0.013 g O<sub>2</sub> m<sup>-3</sup>h<sup>-1</sup> at 20 °C. This value is within the range of measured values for the Chesapeake Bay between 0.01 and 0.04 g O<sub>2</sub> m<sup>-3</sup>h<sup>-1</sup> [29]. We estimated the mean respiration rate  $R^{20}$  based on the minimum root-mean-square error (RMSE) between observed and modeled DO. The estimated net consumption rate at 20 °C ranges from 0.15 to 0.36 g O<sub>2</sub> m<sup>-3</sup>d<sup>-1</sup>. Higher respiration rates are located in the upper Bay. The results are within the same range of observations [29]. The results show a good agreement between the modeled DO and observations, with a mean RMSE ranging from 0.73 to 0.92. The difference between modeled DO and observations can be attributed to the use of constant net consumption rate of  $R^{20}$ . Because of interannual variations of nutrient loadings,  $R^{20}$  has a high interannual version, which is highly correlated with the nutrient loading [13]. It is expected that the modeled DO will be improved if temporally varying net consumption rates are used.

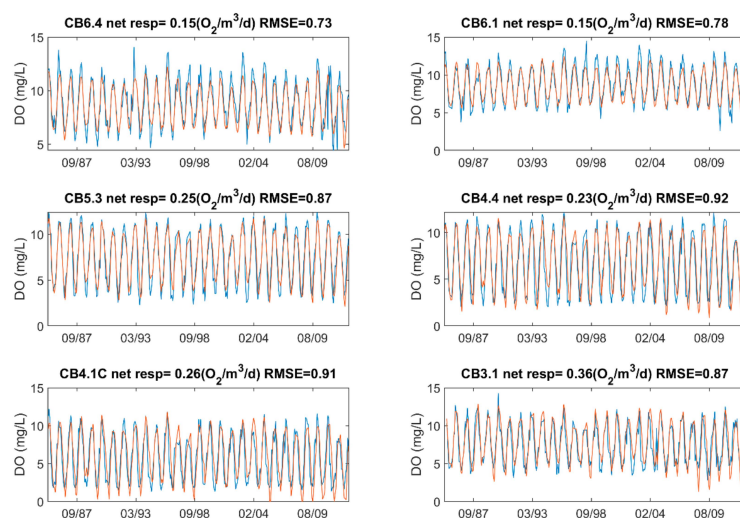


**Figure 5.** Comparisons of model results of vertical mean DO against observations at selected stations (blue lines are observations and red lines are model results).

## 4. Discussion

### 4.1. Transport Timescales

The simplified models provide a Lagrangian perspective on DO variations. DO at a location can be estimated as the superimposition of the DO transport from the upper stream and downstream, and from the surface (Equation (7)). In the context of a water parcel, the impact on DO due to transport can be divided into three components: transport from the surface ( $Q_v, \tau_v$ ), upstream freshwater ( $Q_u, \tau_u$ ), and downstream saltwater ( $Q_d, \tau_d$ ), as depicted in Figure 6. In particular, the computation of  $\tau_v$  encompasses all water parcels that have encountered the surface since the last time during the transport, which may result from direct vertical mixing, lateral transport due to lateral circulation, and transport from both the upstream and downstream locations. When water parcels enter the estuary through upstream or downstream boundaries, only a fraction of the water parcels are transported to the specified location without encountering the surface, and the rest of them reach the surface during the transport process. Upon contact with the surface, the DO of the water parcels is mixed up with the DO near the surface, and the age of the water parcels resets to zero. Subsequently, these water parcels are treated as the surface water parcels in the calculation. By understanding the pathways and the transport times of these three water ages, we can estimate the DO consumption during their transport, thus estimating DO at each location. Our simplified equation captures these distinctions among water parcels, despite being derived from a simplified model. DO consumption is quantified by freshwater, saltwater, and vertical transport ages to represent these three types of water parcels.

We computed the water age using CART, which provides an accurate estimate of the water age including all the dynamic processes, variations of bathymetry, and forcings. In practice, the characteristics of these timescales can also be estimated based on mean dynamic conditions or characteristics. The freshwater age at location  $x$  can be estimated by  $x/u_A$ , where  $u_A$  is the cross-section averaged mean velocity (i.e.,  $Q/A$ , where  $Q$  is discharge and  $A$  is cross-section area). The exchange flow can be scaled by the gravitational flow  $U_E$  and estimated as  $(L - x)/U_E$ , where  $L$  is the length of the estuary,  $U_E = \frac{g\beta S_x H^3}{48K_M}$  [15],  $S_x$  is the horizontal salinity gradient,  $K_M$  is vertical eddy viscosity,  $H$  is depth, and  $\beta = 7.7 \times 10^{-4}$ .  $K_M$  can be estimated as  $K_M = K(1 + 10R_i)^{-1/2} \approx 0.316 K$ ,  $K = C_D H U$ , where  $C_D$  is the drag coefficient,  $U$  is the tidal averaged velocity, and  $R_i$  is the Richardson number [30]. The vertical exchange time can be estimated as  $\tau_v = H^2/K_s$  [30], where  $K_s = K(1 + 3.3R_i)^{-1/2} \approx 0.167 K$ .

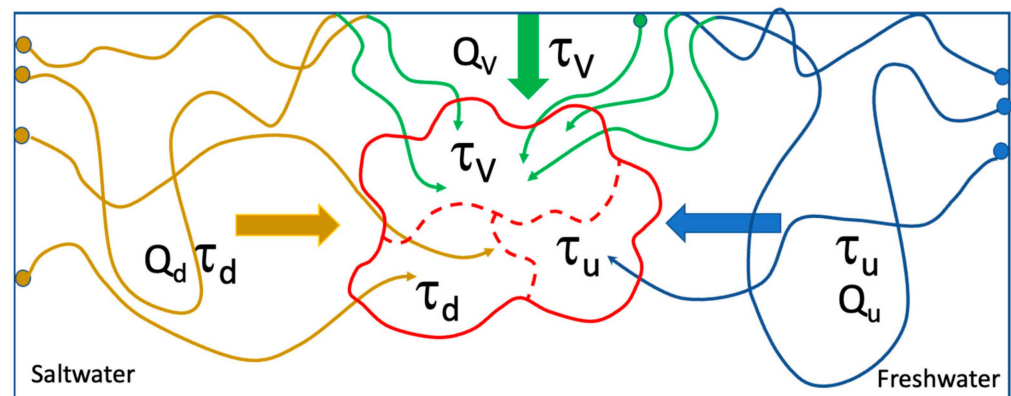


**Figure 6.** A diagram illustrating the pathways of water parcels during transport.

#### 4.2. Hypoxia Assessment

If we assume that the DO at the boundaries and surface reaches saturation,  $O_{sa}$ , then Equation (7) can be written as:

$$O = O_{sa} - \tau_v R_N (1 - e^{-\frac{\tau_u}{\tau_v}} - e^{-\frac{\tau_d}{\tau_v}}) \tag{14}$$

We can define a combined timescale  $\tau_T = \tau_v (1 - e^{-\frac{\tau_u}{\tau_v}} - e^{-\frac{\tau_d}{\tau_v}})$ , and the DO concentration at location  $x$  can be expressed as:

$$O(x) = \max((O_{sa}(x) - \tau_T(x) R_N(x)), 0) \tag{15}$$

where all variables vary with location. If water moves much faster than  $\tau_v$  ( $\tau_d$  or  $\tau_u \ll \tau_v$ ), DO will approach saturation conditions (or DO conditions at the boundary), and there is not enough consumption time for DO to be depleted.

If hypoxia is defined as less than  $2 \text{ g O}_2 \text{ m}^{-3}$ , the combined transport timescale should satisfy the following condition without hypoxia:

$$\tau_T \leq \frac{O_{sa} - 2}{R_N} \tag{16}$$

This equation provides a simple assessment of DO conditions at any location. For example, if  $O_{sa} = 7 \text{ g m}^{-3}$  in summer,  $R_N$  is on the order of 0.3 per day [13] and requires  $\tau_T \leq 16.67$  days to satisfy the conditions without hypoxia. The mean  $\tau_T$  is about 20 d at Station CB4.1C and is about 14 d at Station CB5.2 (Figure 4). This suggests that the mean DO is less than  $2 \text{ g O}_2 \text{ m}^{-3}$  at Station CB4.1C, but it is larger than  $2.0 \text{ g O}_2 \text{ m}^{-3}$  at Station 5.3.

Fennel and Testa [14] compared the residence time and timescales of oxygen consumption and introduced a simple scale for hypoxia conditions as follows:  $\tau_{hyp} = \frac{O_{ini}}{R}$  and  $\gamma = \frac{\tau_{hyp}}{\tau}$  ( $O_{ini}$  is the initial waterbody DO concentration that can be assumed to be under saturation,  $R$  is the net DO consumption rate, and  $\tau$  is residence time). They suggest that a waterbody under hypoxia conditions requires  $\gamma < 1$ . This scale provides a convenient way to evaluate hypoxia conditions in a waterbody. However, this criterion is for anoxia and overlooks the difference between residence time and vertical exchange time when controlling DO replenishment. It works for a small waterbody with a short residence time or a system where the residence time is on the same order of  $\tau_v$ . For a large estuary with long residence times, vertical replacement is the dominant method of DO replacement through physical transport processes, such as the Chesapeake Bay (mean  $\tau = 180 \text{ d}$  [31]) and the James River (mean  $\tau = 90 \text{ d}$  [32]). Therefore, the residence time  $\tau$  needs to be carefully defined. For example, in the James River, a tributary of the Chesapeake Bay, the average net DO consumption rate in the water column is about  $0.3 \text{ g O}_2 \text{ m}^{-3} \text{ d}^{-1}$  [10], mean residence time is 90 d, and the residence time during high flow is about 40 d [32]. Assuming that summer saturation DO concentration is  $7 \text{ g O}_2 \text{ m}^{-3}$ , and residence time is 40 d, it gives  $\gamma < 0.58 < 1$ , indicating a condition favoring hypoxia according to the scaling by Fennel and Testa’s criteria [14]. However, hypoxia does not occur in the James River due to short vertical exchange time and the presence of strong gravitational circulation near the mouth [3], which suggests that using residence time as a measure is not adequate for large estuaries.

Using Equation (13), we can find the required conditions when DO is zero ( $O = 0$ , anoxia condition), and  $\gamma$  can be written as

$$\gamma = \frac{O_{sa}}{R\tau_v} = \frac{1}{1 + \frac{\tau_v}{\tau}} < 1 \text{ if } \tau_v \ll \tau \text{ or } \gamma = \frac{O_{sa}}{R\tau} = \frac{1}{1 + \frac{\tau}{\tau_v}} < 1 \tau \ll \tau_v \tag{17}$$

This gives  $\gamma < 1$  for anoxia conditions. It can be seen that a more accurate estimation is to use different timescales with consideration of dominant hydrodynamic conditions causing low DO when using this criterion. Note that  $\tau_v$  is about 10 d in the James [10], which

is less than residence time  $\tau$  in the James. Using the same values of  $R_N$  ( $0.3 \text{ g O}_2 \text{ m}^{-3}\text{d}^{-1}$ ) and saturation DO concentration ( $7.0 \text{ g O}_2 \text{ m}^{-3}$ ), we obtain  $\gamma = 2.3 > 1$ . This suggests there are no anoxia conditions in the James.

For hypoxia conditions defined as DO concentration  $\leq 2 \text{ g O}_2 \text{ m}^{-3}$ , a criterion for hypoxia can be expressed as:

$$\gamma' = \frac{O_s - 2}{R\tau_v} = < 1 \text{ or } \gamma' = \frac{O_s - 2}{R\tau} < 1. \quad (18)$$

This criterion can also be applied to a section of an estuary. For example, in the middle of Chesapeake Bay where influence from both upstream and downstream are minimum,  $R \approx 0.3 \text{ g O}_2 \text{ m}^{-3}\text{d}^{-1}$ ,  $\tau_v$  is about 20 d, and  $\tau > 100$  d in summer (Figure 5, Stations CB4.4 and CB4.1C), so that  $\gamma' = 0.83$ , which indicates that hypoxia is favored. On the other hand, in the lower Bay (Figure 5, Stations CB6.4, CB6.1, and CB5.3),  $\tau_v$  is less than 10 d, and  $\tau$  is less than 50 d, leading to  $\gamma' > 1$ , which indicates that hypoxia is not favored if measured by the mean DO concentration.

It should be noted that the criteria presented here are for assessing the vertically averaged DO conditions for a system. Since the vertically mean DO concentration is typically higher than the bottom DO concentration, the bottom water can experience hypoxia conditions if the estuary is stratified at a certain location even though the mean DO concentration is high. For the estimation of bottom DO concentration in an estuary, the vertical exchange time at the bottom should be used in Equations (17) and (18) based on the two-layer model developed by Shen et al. [10]. On the other hand, if the gradational circulation is strong at the location near the mouth, which is shorter than vertical exchange time, Equation (16) should be used for the assessment of DO conditions at the location of concern.

## 5. Conclusions

To understand the impact of hydrodynamics and biochemical processes on hypoxia in rivers and estuaries, we introduced timescales representing these processes to quantify variations in DO concentrations. These timescales serve as a common currency [9] for assessing the onset of hypoxia and enable cross-system comparisons. Derived from a simple model, these timescales offer insights into the intricate interplay between DO consumption and dynamic replenishment without sacrificing generality. The resulting relationship provides a Lagrangian perspective, enhancing our understanding of the physical processes involved in DO consumption and replenishment.

Water parcels at a specific location are categorized into three components: those transported from the surface, from upstream freshwater, and from downstream saltwater. In particular, the component of surface-transported water parcels encompasses all water parcels that have encountered the surface during transport, which may result from direct vertical mixing, lateral transport due to lateral circulation, and transport from both the upstream and downstream locations. Water parcels transported from upstream and downstream boundaries without contacting the surface are classified as freshwater and saltwater parcels, respectively. Water ages are computed to represent the transport timescales for these three types of water parcels based on CART, providing accurate estimates of transport times that account for all the dynamic transport processes. The estimation of DO concentration at a location of concern is achieved based on the established relationships, computed water ages, and estimated net DO consumption rates. Applying the simple model with timescales computed for the Chesapeake Bay, our results demonstrate accurate predictions of DO levels over 26 years at multiple stations. With an appropriate estimate of temporal variations of the net DO consumption rate, DO estimation can be improved.

We have introduced a simple model aimed at providing a general understanding of the key processes controlling hypoxia in estuaries while acknowledging the many assumptions inherent in the model. To address specific ecological problems and answer management questions, complex ecosystem models are needed for different temporal

and spatial scales. However, our simple model approach provides criteria that allow us to conduct cross-system comparisons for the potential formation of hypoxia conditions. Criteria for cross-system comparison to determine hypoxia and anoxia are established based on transport timescales, highlighting the critical importance of these timescales in using such criteria. Our study reveals that the hypoxia/anoxia status of a river or estuary system is determined by the timescales of vertical exchange, freshwater transport, saltwater transport, and net DO consumption rate. The shortest timescale that determines the DO replenishment is the dominant factor physically controlling DO dynamics in estuaries. The interplay between DO consumption and dynamic replenishment emerges as the primary determinant of hypoxia in an estuarine environment.

**Author Contributions:** Conceptualization, J.S.; Methodology, J.S. and Q.Q.; Investigation, J.S. and Q.Q.; Writing—original draft, J.S.; Writing—review & editing, J.S. and Q.Q. All authors have read and agreed to the published version of the manuscript.

**Funding:** This research received no external funding.

**Data Availability Statement:** The observation DO data is available at <https://www.chesapeakebay.net/what/downloads/cbp-water-quality-database-1984-present> (accessed on 20 March 2024). The processed age data refer to reference [13]. No new data was generated.

**Acknowledgments:** We thank Lisa Lucas for many constructive discussions. We are grateful to Jiabi Du for providing model results for age calculations in the Chesapeake Bay. We thank the two anonymous reviewers for their constructive comments and suggestions that have improved the manuscript.

**Conflicts of Interest:** The authors declare no conflicts of interest.

## References

- Diaz, R.J. Overview of hypoxia around the world. *J. Environ. Qual.* **2001**, *30*, 275–281. [[CrossRef](#)] [[PubMed](#)]
- Officer, C.B.; Biggs, R.B.; Taft, J.L.; Cronin, L.E.; Tyler, M.A.; Boynton, W.R. Chesapeake bay anoxia: Origin, development, and significance. *Science* **1984**, *223*, 22–27. [[CrossRef](#)]
- Kuo, A.Y.; Neilson, B.J. Hypoxia and salinity in Virginia estuaries. *Estuaries* **1987**, *10*, 277–283. [[CrossRef](#)]
- Cloern, J. Our evolving conceptual model of the coastal eutrophication problem. *Mar. Ecol. Prog. Ser.* **2001**, *210*, 223–253. [[CrossRef](#)]
- Boicourt, W.C. Influence of circulation processes on dissolved oxygen in the Chesapeake Bay. In *Oxygen Dynamics in Chesapeake Bay: A Synthesis of Recent Research*; Smith, D.E., Leffler, M., Mackiernan, G., Eds.; Maryland Sea Grant Publication: College Park, MD, USA, 1992; pp. 7–59.
- Hagy, J.D.; Boynton, W.R.; Keefe, C.W.; Wood, K.V. Hypoxia in Chesapeake Bay, 1950–2001: Long-term change in relation to nutrient loading and river flow. *Estuaries* **2004**, *27*, 634–658. [[CrossRef](#)]
- Sanford, L.P.; Sellner, K.G.; Breitburg, D.L. Covariability of dissolved oxygen with physical processes in the summertime Chesapeake Bay. *J. Mar. Res.* **1990**, *48*, 567–590. [[CrossRef](#)]
- Scully, M.E. Wind modulation of dissolved oxygen in Chesapeake Bay. *Estuaries Coasts* **2010**, *33*, 1164–1175. [[CrossRef](#)]
- Lucas, L.V.; Deleersnijder, E. Timescale methods for simplifying, understanding and modeling biophysical and water quality processes in coastal aquatic ecosystems: A review. *Water* **2020**, *12*, 2717. [[CrossRef](#)]
- Shen, J.; Hong, B.; Kuo, A.Y. Using timescales to interpret dissolved oxygen distributions in the bottom waters of Chesapeake Bay. *Limnol. Oceanogr.* **2013**, *58*, 2237–2248. [[CrossRef](#)]
- Shen, J.; Du, J.; Lucas, L.V. Simple relationships between residence time and annual nutrient retention, export, and loading for estuaries. *Limnol. Oceanogr.* **2022**, *67*, 918–933. [[CrossRef](#)]
- Lucas, L.V.; Thompson, J.K.; Brown, L.R. Why are diverse relationship observed between phytoplankton biomass and transport time? *Limnol. Oceanogr.* **2009**, *54*, 381–390. [[CrossRef](#)]
- Du, J.; Shen, J. Decoupling the influence of biological and physical processes on the dissolved oxygen in the Chesapeake Bay. *J. Geophys. Res. Oceans* **2015**, *120*, 78–93. [[CrossRef](#)]
- Fennel, K.; Testa, J.M. Biogeochemical controls on coastal hypoxia. *Annu. Rev. Mar. Sci.* **2018**, *11*, 105–130. [[CrossRef](#)]
- Hansen, D.V.; Rattray, M. Gravitational circulation in straits and estuaries. *J. Mar. Res.* **1965**, *23*, 104–122. [[CrossRef](#)]
- MacCready, P. Toward a unified theory of tidally-averaged estuarine salinity structure. *Estuaries* **2004**, *27*, 561–570. [[CrossRef](#)]
- Lin, J.; Xie, L.; Pietrafesa, L.J.; Shen, J.; Mallin, M.A.; Durako, M.J. Dissolved oxygen stratification in two micro-tidal partially-mixed estuaries. *Estuar. Coast. Shelf Sci.* **2006**, *70*, 423–437. [[CrossRef](#)]
- Deleersnijder, E.; Campin, J.-M.; Delhez, E.J. The concept of age in marine modelling: I. Theory and preliminary model results. *J. Mar. Syst.* **2001**, *28*, 229–267. [[CrossRef](#)]

19. Delhez, É.; Lacroix, G.; Deleersnijder, É. The age as a diagnostic of the dynamics of marine ecosystem models. *Ocean Dyn.* **2004**, *54*, 221–231. [[CrossRef](#)]
20. Vollenweider, R.A. Input-output models with special reference to the phosphorus loading concept in limnology. *Schweiz. Z. Hydrol.* **1975**, *37*, 53–84.
21. Hamrick, J.M. *A Three-Dimensional Environmental Fluid Dynamics Computer Code: Theoretical and Computational Aspects*; Special Report in Applied Marine Science and Ocean Engineering. No. 317; Virginia Institute of Marine Science, College of William and Mary: Williamsburg, VA, USA, 1992.
22. Hong, B.; Wang, G.; Xu, H.; Wang, D. Study on the transport of terrestrial dissolved substances in the Pearl River Estuary Using Passive Tracers. *Water* **2020**, *12*, 1235. [[CrossRef](#)]
23. Gustafsson, K.E.; Bendtsen, J. Elucidating the dynamics and mixing agents of a shallow fjord through age tracer modelling. *Estuar. Coast. Shelf Sci.* **2007**, *74*, 641–654. [[CrossRef](#)]
24. Deleersnijder, E.; Draoui, I.; Lambrechts, J.; Legat, V.; Mouchet, A. Consistent boundary conditions for age calculations. *Water* **2020**, *12*, 1274. [[CrossRef](#)]
25. Da, F.; Friedrichs, M.A.M.; St-Laurent, P. Impacts of atmospheric nitrogen deposition and coastal nitrogen fluxes on oxygen concentrations in Chesapeake Bay. *J. Geophys. Res. Ocean.* **2018**, *123*, 5004–5025. [[CrossRef](#)]
26. Thomann, R.V.; Mueller, J.A. *Principles of Surface Water Quality Modeling and Control*; Harper and Row: Manhattan, NY, USA, 1987.
27. Cowan, J.L.W.; Boynton, W.R. Sediment-water oxygen and nutrient exchanges along the longitudinal axis of Chesapeake Bay: Seasonal patterns, controlling factors and ecological significance. *Estuaries* **1996**, *19*, 562–580. [[CrossRef](#)]
28. Boynton, W.; Kemp, W. Nutrient regeneration and oxygen consumption by sediments along an estuarine salinity gradient. *Mar. Ecol. Prog. Ser.* **1985**, *23*, 45–55. [[CrossRef](#)]
29. Smith, E.; Kemp, W. Seasonal and regional variations in plankton community production and respiration for Chesapeake Bay. *Mar. Ecol. Prog. Ser.* **1995**, *116*, 217–231. [[CrossRef](#)]
30. Munk, W.H.; Anderson, E.R. Notes on the theory of the thermocline. *J. Mar. Res.* **1948**, *7*, 276–295.
31. Nixon, S.W.; Ammerman, J.W.; Atkinson, L.P.; Berounsky, V.M.; Billen, G.; Boicourt, W.C.; Boynton, W.R.; Church, T.M.; DiToro, D.M.; Elmgren, R.; et al. The fate of nitrogen and phosphorus at the land-sea margin of the North Atlantic Ocean. *Biogeochemistry* **1996**, *35*, 141–180. [[CrossRef](#)]
32. Shen, J.; Lin, J. Modeling study of the influences of tide and stratification on age of water in the tidal James River. *Estuar. Coast. Shelf Sci.* **2006**, *68*, 101–112. [[CrossRef](#)]

**Disclaimer/Publisher’s Note:** The statements, opinions and data contained in all publications are solely those of the individual author(s) and contributor(s) and not of MDPI and/or the editor(s). MDPI and/or the editor(s) disclaim responsibility for any injury to people or property resulting from any ideas, methods, instructions or products referred to in the content.